Journal of Sound and Vibration (1997) **207**(3), 393–401

PRIMARY RESONANCE OF A HARMONICALLY FORCED OSCILLATOR WITH A PAIR OF SYMMETRIC SET-UP ELASTIC STOPS

H. Y. Hu

Institute of Vibration of Engineering Research, Nanjing University of Aeronautics & Astronautics, 210016 Nanjing, People's Republic of China

(*Received* 15 *March* 1996, *and in final form* 8 *May* 1997)

The primary resonance and the stability of a harmonically forced oscillator with a pair of symmetric set-up elastic stops are studied by means of the average approach. It is found that the set-up elastic stops greatly increase the complexities of the primary resonance as follows. Four kinds of persistent primary resonance and three critical cases exist. The motion of many of the persistent resonances becomes unstable when it begins to touch the set-up elastic stops with decrease of the excitation frequency. Moreover, there coexist three stable periodic motions and two unstable periodic motions at certain combinations of system parameters.

1. INTRODUCTION

The elastic components in mechanical systems are often preloaded due to a variety of reasons. A simple, but widely used model in vibration control, vibration machinery and so on is a harmonically forced oscillator with a pair of symmetrical set-up elastic stops as shown in Figure 1. As shown in Figure 2(a), the elastic restoring force in such an oscillator is piecewise linear and undergoes a finite jump equal to the preload when the mass touches the set-up elastic stop.

In the past decade, the dynamics of piecewise-linear oscillators has been intensively studied. For instance, Shaw [1] revealed the complex dynamics of a forced oscillator impacting on two rigid walls by using the modern theory of dynamical systems. Cone and Zadoks [2] studied the similar vibro-impact system with friction damping [2]. These studies were based on a simultaneous restitution model, which neglects the impact time so that the restoring force goes to infinity on impact as shown in Figure 2(b). To take the impact time into account, many other studies have been based on the model of elastic stops having the continuous, but piecewise-linear restoring force shown in Figure 2(c). For example, Natsiavas [3] developed a numerical scheme to locate the periodic motions of harmonically forced trilinear oscillators and discussed the stability of the periodic motions [3]. Hu [4, 5] analyzed the grazing induced bifurcations of the same oscillator.

Compared with these two types of models, the preloaded elastic stops in the oscillator results in more complicated restoring force, and hence the discontinuous vector field of the differential equation of motion. However, little attention has been paid to the qualitative changes of the system dynamics caused by the preload since the early study of Den Hartog [6] on a harmonically forced, undamped oscillator with a pair of set-up springs. To the author's knowledge, only Mahfouz and Badrakhan [7] numerically studied the chaotic motion of similar oscillators in the past decade.

0022–460X/97/430393 + 09 $25.00/0/sv971139

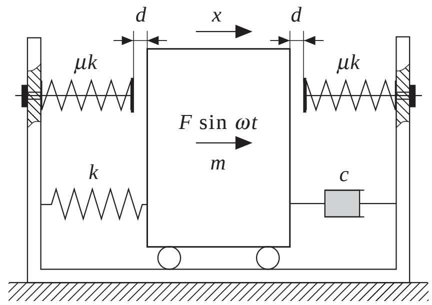

Figure 1. A harmonically forced oscillator with a pair of symmetric set-up elastic stops.

The primary aim of this paper is to reveal the effect of the set-up elastic stops on the qualitative changes of the primary resonance of a harmonically forced oscillator with clearance.

2. STEADY-STATE MOTION OF PRIMARY RESONANCE

Consider the harmonically forced oscillator with a pair of symmetric set-up elastic stops as shown in Figure 1. The governing equation of motion of the system is

$$m\ddot{x} + c\dot{x} + k[x + \mu g(x)] = F \sin \omega t \tag{1}$$

where m, c, k, F, ω and μ are positive parameters denoting the mass quantity, the linear damping coefficient, the linear stiffness coefficient, the excitation amplitude, the excitation frequency and the ratio of the stiffness of an elastic stop to the linear stiffness, respectively. Furthermore, $\mu k g(x)$ denotes the restoring force of the symmetric set-up elastic stops with clearance d and set-up amount e

$$g(x) = \begin{cases} 0, & |x| \leqslant d \\ x + (e - d)\,\mathrm{sgn}\, x, & |x| > d \end{cases} \tag{2}$$

By scaling equations (1) and (2) with the dimensionless time, displacement and parameters as follows

$$\tau = \sqrt{\frac{m}{k}}\, t, \qquad y = \frac{x}{d}, \qquad \zeta = \frac{c}{2\sqrt{mk}}, \qquad \delta = \frac{e}{d} \qquad f = \frac{F}{kd}, \qquad \lambda = \omega\sqrt{\frac{m}{k}} \tag{3}$$

one obtains the dimensionless differential equation of motion

$$y'' + 2\zeta y' + y + \mu h(y) = f \sin \lambda\tau \tag{4}$$

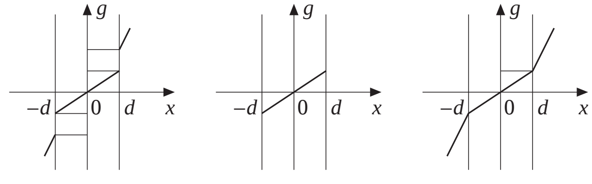

Figure 2. The elastic restoring force of three kinds of piecewise-linear oscillators.

where

$$h(y) = \begin{cases} 0, & |y| \leqslant 1 \\ y + (\delta - 1)\,\mathrm{sgn}\, y, & |y| > 1 \end{cases} \tag{5}$$

and $()'$ denotes the derivative with respect to τ.

To gain insight into the primary resonance of the system through analytic approach, one confines the study to the case of weak nonlinearity, small damping and soft excitation

$$\mu = \mathcal{O}(\varepsilon), \qquad 2\zeta = \mathcal{O}(\varepsilon), \qquad |\lambda^2 - 1| = \mathcal{O}(\varepsilon), \qquad f = \mathcal{O}(\varepsilon), \qquad 0 < \varepsilon \ll 1 \tag{6}$$

and rewrites equation (4) as

$$y'' + \lambda^2 y = (\lambda^2 - 1)y - \mu h(y) - 2\zeta y' + f \sin \lambda\tau \tag{7}$$

Thus, the right hand of equation (7) is of order ε.

Using the average approach, one can truncate the primary resonance to the first order of ε

$$y(\tau) = \alpha(\tau) \sin[\lambda\tau + \varphi(\tau)] \tag{8}$$

and derive a set of autonomous differential equations that govern the time varying amplitude $\alpha(\tau)$ and phase $\varphi(\tau)$

$$\begin{cases} \alpha' = -(1/2\lambda)\,(2\zeta\lambda\alpha + f \sin\varphi) \\ \varphi' = -(1/2\lambda\alpha)\{\alpha[\lambda^2 - 1 - p(\alpha)] + f\cos\varphi\} \end{cases} \tag{9}$$

where

$$p(\alpha) = \begin{cases} 0, & |\alpha| \leqslant 1 \\ (\mu/\pi)\,[\pi - 2\theta + (2\delta - 1)\sin 2\theta], & |\alpha| > 1 \end{cases} \tag{10}$$

$$\theta \equiv \arcsin(1/\alpha) \in (0, \pi/2] \tag{11}$$

The steady-state motion of the primary resonance yields

$$\begin{cases} 2\zeta\lambda\alpha + f\sin\varphi = 0 \\ \alpha[\lambda^2 - 1 - p(\alpha)] + f\cos\varphi = 0 \end{cases} \tag{12}$$

There follows the equations of amplitude and phase, respectively

$$\begin{cases} \alpha^2\{[\lambda^2 - 1 - p(\alpha)]^2 + (2\zeta\lambda)^2\} - f^2 = 0 \\ \tan\varphi - 2\zeta\lambda/[\lambda^2 - 1 - p(\alpha)] = 0 \end{cases} \tag{13}$$

As the amplitude equation here is a quadratic equation of λ^2, it is easy to find whether the equation has a pair of positive roots, a unique positive root or no positive root for any given amplitude α. So, one can readily determine the amplitude–frequency curve. Then, substituting α and the corresponding λ into the phase equation, one obtains the phase–frequency curve.

3. STABILITY ANALSYSIS

As the small amplitude linear vibration is asymptotically stable, one can focus on the stability of non-linear vibration with large amplitude only, i.e., the case of $\alpha > 1$. For a small disturbance $(\varDelta\alpha, \varDelta\varphi)$ to the steady-state motion (α, φ), one has a set of linear, time-invariant, variational differential equations from equation (9)

$$\begin{bmatrix} \varDelta\alpha' \\ \varDelta\varphi' \end{bmatrix} = J \begin{bmatrix} \varDelta\alpha \\ \varDelta\varphi \end{bmatrix} \equiv \begin{bmatrix} J_{11} & J_{12} \\ J_{21} & J_{22} \end{bmatrix} \begin{bmatrix} \varDelta\alpha \\ \varDelta\varphi \end{bmatrix} \tag{14}$$

The steady-state motion of the primary resonance is asymptotically stable if and only if both of the eigenvalues of the Jacobian J have negative real parts.

As shown in Appendix A.1, the Jacobian J and the corresponding determinant are as follows

$$J = \begin{bmatrix} -\zeta & -(f/2\lambda)\cos\varphi \\ \dfrac{f}{2\lambda\alpha^2}\cos\varphi - \dfrac{2\mu}{\pi\lambda\alpha^2\cos\theta}[(2\delta-1)\cos^2\theta - \delta] & -\zeta \end{bmatrix} \tag{15}$$

$$\det J = (f/\lambda^2\alpha^2)\{f/4 - (\mu\cos\varphi/\pi\cos\theta)[(2\delta-1)\cos^2\theta - \delta]\} \tag{16}$$

In what follows all possible parameter combinations that result in the unstable primary resonance are analyzed. According to $\operatorname{tr} J = -2\zeta < 0$ and the Hurwitz theorem, the necessary and sufficient condition for the unstable primary resonance is

$$\det J = (f/\lambda^2\alpha^2)\{f/4 - (\mu\cos\varphi/\pi\cos\theta)[(2\delta-1)\cos^2\theta - \delta]\} < 0 \tag{17}$$

For brevity, one defines a new variable

$$\beta \equiv \beta(\alpha) \equiv \cos\theta = \sqrt{1 - 1/\alpha^2}, \qquad \alpha \in (1, +\infty) \tag{18}$$

so that condition (17) becomes

$$q(\beta) \equiv [(2\delta-1)\cos\varphi]\beta^2 - (\pi f/4\mu)\beta - \delta\cos\varphi > 0 \tag{19}$$

Because β increases monotonically in the interval (0, 1) with $\alpha \in (1, +\infty)$, the condition (17) for the unstable primary resonance when $\alpha > 1$ is equivalent to condition (19) when β, the solution of inequality (19), falls into the interval (0, 1).

The case of $(2\delta - 1)\cos\varphi \neq 0$ is first considered and inequality (19) rewritten as

$$q(\beta) = [(2\delta-1)\cos\varphi](\beta - \beta_1)(\beta - \beta_2) > 0 \tag{20}$$

where

$$\beta_{1,2} = [1/8(2\delta-1)\cos\varphi](\pi f/\mu \mp \sqrt{\varDelta}) \tag{21}$$

are the two roots of $q(\beta) = 0$ and

$$\varDelta \equiv (\pi f/\mu)^2 + 64\delta(2\delta-1)\cos^2\varphi \tag{22}$$

When $0 < \beta_1 < 1$ or $0 < \beta_2 < 1$, the corresponding resonance amplitudes are

$$\alpha_r = \sqrt{1/(1-\beta_r^2)}, \quad r = 1, 2 \tag{23}$$

Now one classifies the positive solutions for inequality (20) as follows.

(a) $2\delta - 1 < 0$, $\cos\varphi > 0$

If $\varDelta < 0$, β_1 and β_2 are a pair of conjugate complex numbers. As shown in Figure 3(a), the curve $q = q(\beta)$ is in the lower-half plane and inequality (20) never holds. If $\varDelta \geqslant 0$, then

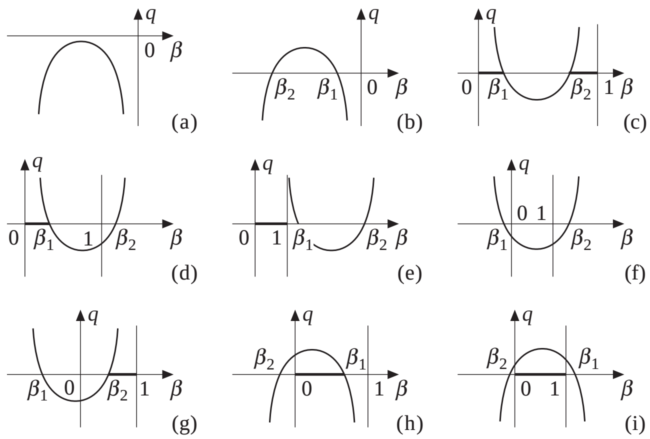

Figure 3. Various solutions for inequality (20).

the curve $q = q(\beta)$ intersects the axis $q = 0$ at $\beta_2 \leqslant \beta_1 < 0$ as shown in Figure 3(b). The solution β of inequality (20) yields $\beta_2 < \beta < \beta_1 < 0$. No matter what case happens, the primary resonance is asymptotically stable.

(b) $2\delta - 1 < 0$, $\cos\varphi < 0$

If $\Delta < 0$, β_1 and β_2 are a pair of conjugate complex numbers again. However, the curve $q = q(\beta)$ is in the upper-half plane and inequality (20) holds for arbitrary β. Hence, the resonance is always unstable when $\alpha > 1$.

If $\Delta \geqslant 0$, then $0 < \beta_1 \leqslant \beta_2$. There exist three possible kinds of positive solutions for inequality (20) as the thick line segments shown in Figure 3(c), Figure 3(d) and Figure 3(e), respectively.

(i) $0 < \beta < \beta_1$ and $\beta_2 < \beta < 1$: In this case, the primary resonance is unstable when the amplitude α yields $1 < \alpha < \alpha_1$ or $\alpha_2 < \alpha$. According to $\beta_2 < 1$ and $\Delta > 0$, the corresponding conditions for the system parameters

$$8|\cos\varphi|\sqrt{\delta(1-2\delta)} < \pi f/\mu < 4|\cos\varphi|(1-\delta), \qquad 0 < \delta < \tfrac{1}{3} \tag{24}$$

are derived in Appendix A.2.

(ii) $0 < \beta < \beta_1 < \beta_2$: In this case the primary resonance loses stability when the amplitude increases to $1 < \alpha < \alpha_1$, and then becomes stable when $\alpha > \alpha_1$. From $\beta_1 < 1$ and $\Delta > 0$, the corresponding condition for the system parameters

$$\pi f/\mu > 4|\cos\varphi|(1-\delta) \tag{25}$$

can be similarly determined.

(iii) $0 < \beta < 1 < \beta_1$: If this is the case, the primary resonance is never stable when $\alpha > 1$. From $\beta_1 > 1$ and $\Delta > 0$, the corresponding conditions for system parameters are

$$8|\cos\varphi|\sqrt{\delta(1-2\delta)}| < \pi f/\mu < 4|\cos\varphi|(1-\delta), \qquad \tfrac{1}{3} < \delta < \tfrac{1}{2} \tag{26}$$

(c) $2\delta - 1 > 0$, $\cos\varphi > 0$

It is obvious that $\Delta > 0$ always holds in this case. There follows $\beta_1 < 0 < \beta_2$. If $\beta_2 > 1$, as shown in Figure 3(f), inequality (20) has no solution in interval (0, 1) so that the primary resonance is stable. Otherwise, the positive solution β for inequality (20) yields $\beta_2 < \beta < 1$ as shown in Figure 3(g). Thus, the primary resonance becomes unstable from an asymptotically stable state when $\alpha_2 < \alpha$. According to $\beta_2 < 1$, one can obtain the conditions for the system parameters

$$\pi f/\mu < 4\cos\varphi(\delta - 1), \qquad \delta > 1 \tag{27}$$

(d) $2\delta - 1 > 0$, $\cos\varphi < 0$:

In this case, $\Delta > 0$ is always true. From $\beta_2 < 0 < \beta_1$, the positive solution for inequality (20) should be $0 < \beta < \min(\beta_1, 1)$ as shown in Figure 3(h) and Figure 3(i). There follows a condition for the system parameters corresponding to $\beta_1 < 1$

$$\pi f/\mu > 4\cos\varphi(\delta - 1) \tag{28}$$

On this condition, the primary resonance is unstable when $1 < \alpha < \alpha_1$. Otherwise, it is unstable for all $\alpha > 1$.

Finally, the case of $(2\delta - 1)\cos\varphi = 0$ is discussed. Now, inequality (19) becomes

$$q(\beta) \equiv -(\pi f/4\mu)\beta - \delta\cos\varphi > 0 \tag{29}$$

If $\cos\varphi \geqslant 0$, inequality (29) has no positive solution and the primary resonance is asymptotically stable. Otherwise, $q(\beta) = 0$ has a single root $\overline{\beta} = 4\delta\mu|\cos\varphi|/\pi f > 0$ so that inequality (29) has the positive solution $0 < \beta < \overline{\beta}$. As a result, there exists $\bar{\alpha} > 0$ corresponding to $\overline{\beta}$ such that the primary resonance is unstable when $1 < \alpha < \bar{\alpha}$.

4. PERSISTENT PRIMARY RESONANCE

Summarizing the conditions for unstable resonance derived in section 3, one finds that there exist four kinds of persistent primary resonance and three critical cases for different combinations of δ and f/μ. Although conditions (24–29) contain $\cos\varphi$, all bifurcations of the primary resonance with respect to the excitation frequency happen in the excitation frequency range corresponding to $|\cos\varphi| \approx 1$. So one can classify the resonance according to the combination of δ and f/μ in the first quadrant of their plane. As shown in Figure 4, the quadrant consists of four regions A, B, C and D, where the parameter combinations result in four kinds of persistent resonance respectively. The interface of these regions includes an arc defined by

$$\pi f/\mu = 8\sqrt{\delta(1 - 2\delta)} \tag{30}$$

and two line segments. They serve as three transition sets where the primary resonance is critical in the sense of structural stability.

Given $\zeta = 0{\cdot}01$ and $\mu = 0{\cdot}3$, four amplitude–frequency curves corresponding to typical parameter combinations in regions A, B, C and D are shown in Figure 5, respectively. It is obvious that the amplitude–frequency curve in case A is very similar to that of a system with elastic stops not preloaded. However, when the amplitude increases with decrease

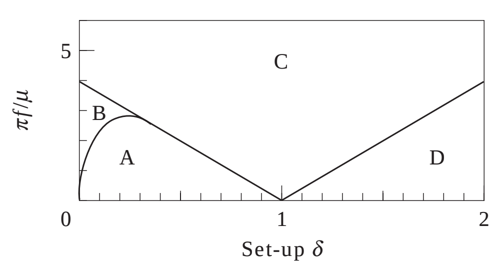

Figure 4. Transition sets and persistence regions of the primary resonance on the plane of system parameters.

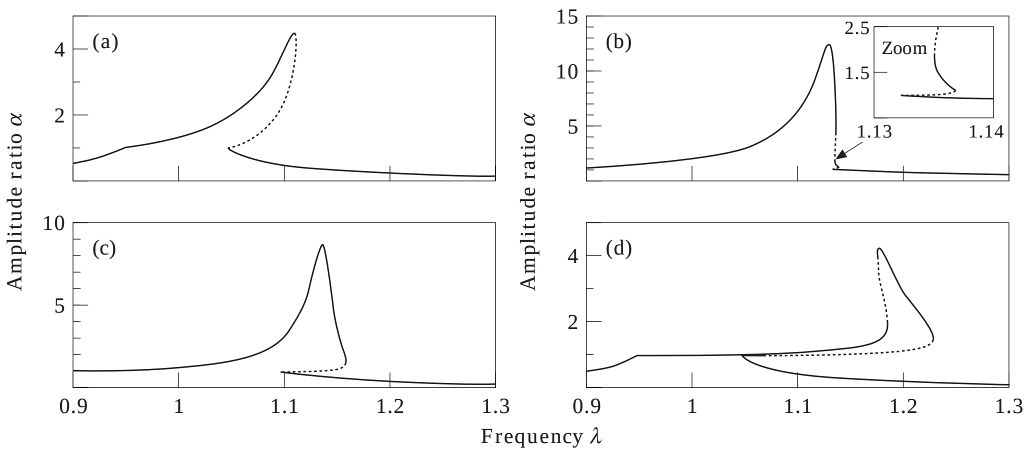

Figure 5. Amplitude–frequency curves of four kinds of persistent primary resonance (—, stable; - - - -, unstable). (a) Case A, $\delta = 0{\cdot}20$, $f = 0{\cdot}10$; (b) Case B, $\delta = 0{\cdot}20$, $f = 0{\cdot}28$; (c) Case C, $\delta = 0{\cdot}75$, $f = 0{\cdot}20$; (d) Case D, $\delta = 2{\cdot}00$, $f = 0{\cdot}10$.

of the excitation frequency, the system motion that just touches the set-up elastic stops will become unstable. This behavior differs from that of a system with elastic stops not preloaded [3–5]. For the parameter combinations in regions B, C and D, the amplitude–frequency curves show more apparent effect of set-up elastic stops on the primary resonance. One of the features of the set-up elastic stops is that the static stiffness of the system becomes hardening first and then softening with increase of the system displacement. The amplitude–frequency curves, therefore, twice change trends. As a result, in cases B and D there coexist three stable periodic motions and two unstable periodic motions in a frequency range.

5. CONCLUSIONS

The preload on the elastic stops in a harmonically forced oscillator gives rise to the following qualitative changes of the primary resonance.

1. The periodic motion that just touches the elastic stops becomes unstable when the amplitude increases with the decrease of the excitation frequency.
2. There are four kinds of persistent primary resonance. Among them, two kinds may have five coexisting periodic motions, two of which are unstable.

ACKNOWLEDGMENTS

This research was supported in part by the National Natural Science Foundation of China and in part by the Trans-Century Training Program Foundation for the Talents of the State Education Commission, China.

REFERENCES

1. S. W. Shaw 1985 *Journal of Applied Mechanics* **52**, 453–464. The dynamics of a harmonically excited system having rigid amplitude constraints.
2. K. M. Cone and R. I. Zadoks 1995 *Journal of Sound and Vibration* **188**, 659–683. A numerical study of an impact oscillator with the addition of dry friction.

3. S. NATSIAVAS 1989 *Journal of Sound and Vibration* **134**, 315–331. Periodic response and stability of oscillators with symmetric trilinear restoring force.
4. H. Y. HU 1995 *Journal of Sound and Vibration* **187**, 485–493. Detection of grazing orbits and incident bifurcations of a forced continuous, piecewise-linear oscillator.
5. H. Y. HU 1995 *Chaos*, *Solitons and Fractals*, **5,** 2201–2212. Simulation complexities in the dynamics of a continuously piecewise-linear oscillator.
6. J. P. DEN HARTOG 1956 *Mechanical Vibrations*. New York: McGraw-Hill.
7. I. A. MAHFOUZ and F. BADRAKHAN 1990 *Journal of Sound and Vibration* **143**, 255–288. Chaotic behavior of some piecewise-linear systems, part I: systems with set-up spring or with unsymmetric elasticity.

APPENDIX

A.1. JACOBIAN AND ITS DETERMINANT

Differentiating the right side of equation (9) with respect to a and φ, one has

$$\begin{cases} J_{11} = (\partial/\partial\alpha)\,[-(1/2\lambda)\,(2\zeta\lambda\alpha + f\sin\varphi)] = -\zeta \\ J_{12} = (\partial/\partial\varphi)\,[-(1/2\lambda)\,(2\zeta\lambda\alpha + f\sin\varphi)] = -(f/2\lambda)\cos\varphi \\ J_{21} = (\partial/\partial\alpha)\{-(1/2\lambda\alpha)\{\alpha[\lambda^2 - 1 - p(a)] + f\cos\varphi\}\} \\ \quad = (f/2\lambda\alpha^2)\cos\varphi + (\mu/\lambda\pi)\,[(2\delta-1)\cos 2\theta - 1]\,\mathrm{d}\theta/\mathrm{d}\alpha \\ J_{22} = (\partial/\partial\varphi)\{-(1/2\lambda\alpha)\{\alpha[\lambda^2 - 1 - p(a)] + f\cos\varphi\}\} = (f/2\lambda\alpha)\sin\varphi \end{cases} \tag{A-1}$$

To evaluate $\mathrm{d}\theta/\mathrm{d}\alpha$ in J_{21}, on can differentiate equation (11) with respect to a

$$\cos\theta\ \mathrm{d}\theta/\mathrm{d}\alpha = -1/\alpha^2 \tag{A-2}$$

Substituting equation (A-2) into J_{21} in equation (A-1) yields

$$\begin{aligned} J_{21} &= (f/2\lambda\alpha^2)\cos\varphi - (\mu/\pi\lambda\alpha^2)\,[(2\delta-1)\cos 2\theta - 1]/\cos\theta \\ &= (f/2\lambda\alpha^2)\cos\varphi - (2\mu/\pi\lambda\alpha^2)\,[(2\delta-1)\cos^2\theta - \delta]/\cos\theta \end{aligned} \tag{A-3}$$

In addition, the first equation in equation (12) gives

$$J_{22} = -\zeta \tag{A-4}$$

Thus, one has

$$\det J = \zeta^2 + f^2\cos^2\varphi/4\lambda^2\alpha^2 - (\mu f\cos\varphi/\pi\lambda^2\alpha^2\cos\theta)\,[(2\delta-1)\cos^2\theta - \delta] \tag{A-5}$$

Using the first equation in equation (12) again, one has

$$f^2\cos^2\varphi = f^2(1 - \sin^2\varphi) = f^2 - 4\zeta^2\lambda^2\alpha^2 \tag{A-6}$$

By substituting it into (A-5), one obtains

$$\det J = (f/\lambda^2\alpha^2)\{f/4 - (\mu\cos\varphi/\pi\cos\theta)\,[(2\delta-1)\cos^2\theta - \delta]\} \tag{A-7}$$

A.2. PROOF OF CONDITION (24)

The inequality $\beta_2 < 1$ is

$$\beta_2 = [1/8\cos\varphi(2\delta-1)]\,(\pi f/\mu + \sqrt{\Delta}) < 1 \tag{A-8}$$

where

$$\Delta \equiv (\pi f/\mu)^2 + 64\delta(2\delta-1)\cos^2\varphi > 0 \tag{A-9}$$

Inequality (A-8) can be rewritten as

$$\sqrt{(\pi f/\mu)^2 + 64\cos^2\varphi(2\delta - 1)} < 8\cos\varphi(2\delta - 1) - \pi f/\mu \tag{A-10}$$

Further simplification of inequality (A-10) results in

$$\pi f/\mu < 4\cos\varphi(\delta - 1) \tag{A-11}$$

Moreover, the right side of inequality (A-10) should be greater than zero so that

$$\pi f/\mu < 8\cos\varphi(2\delta - 1) \tag{A-12}$$

Combining inequalities (A-9), (A-11) and (A-12), one has

$$\begin{aligned} 8|\cos\varphi|\sqrt{\delta(1-2\delta)} < \pi f/\mu &< \min\{4\cos\varphi(\delta - 1), 8\cos\varphi(2\delta - 1)\} \\ &= \begin{cases} 4\cos\varphi(\delta - 1), & 0 < \delta \leqslant \frac{1}{3} \\ 8\cos\varphi(2\delta - 1), & \frac{1}{3} < \delta < \frac{1}{2} \end{cases} \end{aligned} \tag{A-13}$$

However, the inequality

$$8|\cos\varphi|\sqrt{\delta(1-2\delta)} < 8\cos\varphi(2\delta - 1) \tag{A-14}$$

only holds when $0 < \delta < 1/3$ or $\delta > 1/2$. Thus, inequality (A-13) can be simplified as

$$8|\cos\varphi|\sqrt{\delta(1-2\delta)} < \pi f/\mu < 4|\cos\varphi|(1 - \delta), \qquad 0 < \delta < \tfrac{1}{3} \tag{A-15}$$